Age and Gender Differences in Normal Myocardial Adrenergic Neuronal Function Evaluated by Iodine-123-MIBG Imaging

Shinsaku Tsuchimochi, Nagara Tamaki, Eiji Tadamura, Masahide Kawamoto, Toru Fujita, Yoshiharu Yonekura and Junji Konishi

Departments of Nuclear Medicine and Neuropathophysiology, Kyoto University Faculty of Medicine, Kyoto, Japan

Myocardial sympathetic nervous function has been evaluated with ^{123}I-metaiodobenzylguanidine (MIBG) imaging in various cardiac diseases. Heterogeneous distribution of this tracer has been reported. This study was undertaken to assess whether such heterogeneity is related to age and gender. **Methods:** Twenty-nine subjects (18 men, 11 women; age range, 21 to 79 yr; mean age 42 ± 17 yr) with no cardiac disorders were studied. Early (15 min) and late (3–4 hr) planar images were taken, and SPECT images were also obtained 3–4 hr after MIBG injection (111 MBq). The mean counts of the whole heart, mediastinum and the anterior and inferior regions of the heart were obtained to calculate heart-to-mediastinum count ratios, myocardial washout rates and the inferior-to-anterior wall count ratio. On a bull's-eye map of the SPECT images, the left ventricular myocardium was divided into nine sectors to calculate the inferior-to-anterior wall count ratio. **Results:** There were no significant differences in the heart-to-mediastinum count ratio based on age or gender, but there was a significant inverse correlation between the inferior-to-anterior wall count ratio and age ($r = -0.51$ on late planar images and $r = -0.69$ on SPECT; $p < 0.01$ and $p < 0.001$, respectively). This correlation was valid in men ($r = -0.74$ and -0.83, respectively; both $p < 0.001$), but not in women ($r = -0.25$ and -0.34, respectively; p = ns). **Conclusion:** Inferior wall uptake of MIBG decreased with age in individuals without cardiac diseases, especially men. Such age- and gender-related heterogeneity should be considered in the interpretation of MIBG images.

Key Words: myocardial adrenergic function; iodine-123-metaiodobenzylguanidine; single-photon emission computed tomography; cardiac disease

J Nucl Med 1995; 36:969–974

Although knowledge of cardiac adrenergic activity may be of great potential in pathogenetic and prognostic significance in heart failure, the assessment of its function has been difficult to determine in vivo. Radioiodinated meta-iodobenzylguanidine (MIBG), an analog of guanetidine that shares many neuronal transport and storage mechanisms with norepinephrine, has been introduced as an agent for probing adrenergic neuronal function (*1–5*). Noninvasive radionuclide imaging with [^{123}I]MIBG permits regional assessment of efferent adrenergic neuronal function in the heart (*6–18*); however, little is known about the normal distribution of myocardial sympathetic innervation. Gill et al. (*19*) showed heterogenous tracer distribution. On the other hand, some younger subjects show homogeneous tracer distribution, indicating almost homogeneous myocardial sympathetic innervation. We hypothesized that myocardial distribution of MIBG may be related to age and gender. Accordingly, this study was undertaken to correlate myocardial MIBG uptake, washout and distribution with age and gender in normal individuals.

MATERIALS AND METHODS

Subjects

Twenty-nine subjects (18 men and 11 women; age range, 21 to 79 yr; mean age 42 ± 17 yr) were studied (Table 1). Thirteen subjects were healthy volunteers who had no cardiac disorders or any abnormal symptoms. The remaining 16 subjects were patients with malignant diseases including 14 with malignant lymphoma and 2 with postoperative breast cancer. Each patient was imaged before adriamycin therapy. Neither patients nor subjects had cardiac, pulmonary or mediastinal involvement. None of them showed any abnormalities on electrocardiogram, multigated cardiac blood-pool scintigraphy and other examinations. None of them had a history of diabetes mellitus and none had received reserpine, tricyclic antidepressants or other drugs that could interfere with the uptake of MIBG. Informed consent was obtained from each normal volunteer in accordance with guidelines from the Ethical Committee of Kyoto University Faculty of Medicine.

Protocol for MIBG Scintigraphy

To block tracer uptake in the thyroid gland, each subject received 10 mg of potassium iodine 2 days before the investigation and 10 mg daily for 1 or 2 days afterwards. After [^{123}I]MIBG (111 MBq) was injected at rest as an intravenous bolus, the early planar scan was obtained 15 min postinjection with the subject in a supine position. Three to four hours later, both a late planar and SPECT scan were obtained using a gamma camera equipped with

Received Feb. 28, 1994; revision accepted Sep. 12, 1994.

For correspondence or reprints contact: Nagara Tamaki, MD, Department of Nuclear Medicine, Kyoto University Faculty of Medicine, Shogoin Sakyo-ku, Kyoto 606, Japan.

TABLE 1
Subject Characteristics*

	Male	Female	Total
Normal volunteer	11 (7)	2 (2)	13 (9)
Patients with malignant tumor before adriamycin administration	7 (0)	9 (5)	14 (5)
Total	18 (7)	11 (7)	29 (14)

*Number in parentheses denotes subjects younger than 40 years. No patients with malignancy received chemotherapy with adriamycin.

a low-energy, parallel-hole, general-purpose collimator. Planar images were obtained in the anterior view over a 3-min interval 15 min and 3–4 hr after tracer administration. SPECT was performed with data collections of 30–40 sec each, starting in the 45° right anterior oblique projection and finishing in the 45° left posterior oblique projection, after which a series of transaxial images was reconstructed using filtered backprojection (*20*). Short-axis and long-axis slices perpendicular to the cardiac axes were reorganized and a bull's-eye polar map was generated from the apical to basal short-axis slices to show relative tracer distribution in the myocardium (*21*).

Data Processing

Regions of interest (ROI) in the whole heart were set manually on the early and late planar images (Fig. 1A). After correction for the physical decay of ^{123}I, the tracer washout rate from the myocardium was determined over 3–4 hr. On the late planar images, a 10 × 10-mm^2 region in the mediastinum was used to calculate the mean heart-to-mediastinum count ratio (*17,22*). Other ROIs were drawn in the anterior and inferior myocardium on the late images (Fig. 1B) to calculate the inferior-to-anterior wall count ratio (inferior-to-anterior wall count ratio). For quantitative analysis of tracer distribution on the SPECT images, the left ventricular myocardium was divided into nine segments on the polar map display (Fig. 1C). Segment 1 represented the apical wall, segments 2 and 6 were the anterior wall, segments 3 and 7 were the septum, segments 4 and 8 were the inferior wall, and segments 5 and 9 were the lateral free wall. Segments 2–5 were set over the midventricular region and segments 6–9 over the base. The inferior wall to anterior wall count ratio was calculated from the mean counts in each segment.

Statistical Analysis

Data were expressed as the mean ± s.d. A linear regression was carried out between age versus washout rate, the heart-to-mediastinum ratio and the inferior-to-anterior wall count ratio. The Mann-Whitney U-test was used for between-group comparisons. Probability values of less than 0.05 were considered significant.

RESULTS

The mean and standard deviations of the washout rate, the heart-to-mediastinum ratio and the inferior-to-anterior wall count ratio are shown in Tables 2 and 3. These values were not significantly different between normal subjects and those with malignant diseases without cardiac diseases (Table 2). When the subjects were divided into a younger group, less than 40 yr old, and an older group, 40 yr or older, the washout rate and the heart-to-mediastinum count ratio were not significantly different between the two groups. On the other hand, the inferior-to-anterior wall count ratio was significantly smaller in the older group (Fig. 2) than in the younger group (Fig. 3) in both the planar images (0.97 ± 0.14 versus 1.11 ± 0.17; $p < 0.05$) and the SPECT study (0.76 ± 0.17 versus 0.92 ± 0.09; $p < 0.05$). In addition, while there were no gender differences in the

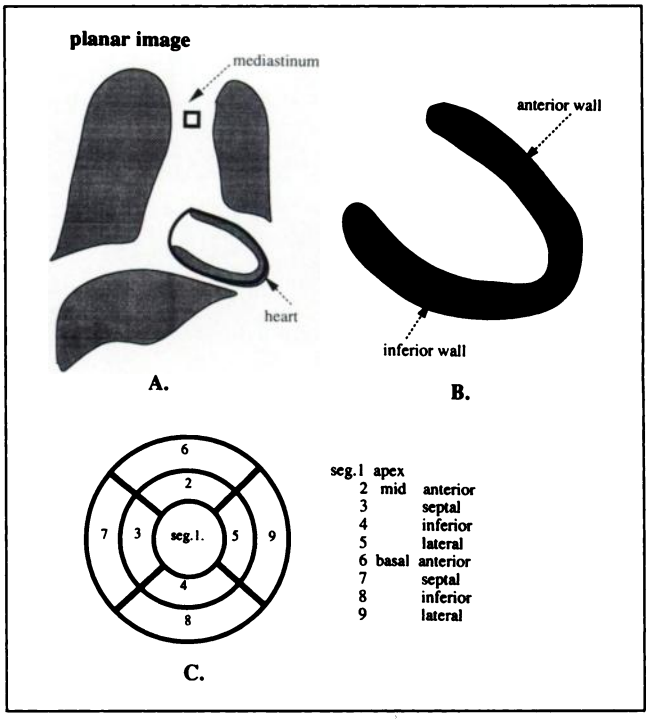

FIGURE 1. Schematic presentation of planar image ROI images and bull's-eye polar map display. (A) The washout rate and heart-to-mediastinum count ratio calculated from the planar image. (B) Inf./Ant. ratio calculated from the planar image. (C) Bull's-eye map with nine sectors.

TABLE 2
Comparison between Normal Volunteers and Patients with Malignancies

	Normal volunteers	Patients with malignant diseases	Significance
Number of subjects	13	16	
Age	31.8 ± 8.1	50.1 ± 17.8	$p < 0.01$
Planar image			
Mean counts			
heart	90.6 ± 13.2	86.2 ± 34.8	ns
mediastinum	31.6 ± 4.5	29.4 ± 9.5	ns
liver	142.5 ± 24.2	150.0 ± 44.3	ns
WR	6.04 ± 21.55	10.80 ± 12.19	ns
H/M	2.87 ± 0.22	2.94 ± 0.49	ns
I/A	1.03 ± 0.14	1.04 ± 0.19	ns
SPECT			
I/A	0.88 ± 0.09	0.81 ± 0.19	ns

WR = washout rate; H/M = heart-to-mediastinum count ratio; I/A = inferior-to-anterior wall count ratio.

TABLE 3
Mean and Standard Deviation Values of Each Parameter with Regard to Age and Gender

	No.	Mean age	Planar image			SPECT
			WR	H/M	I/A	I/A
Age						
<40 yr	14	27.3 ± 4.7	4.6 ± 18.9	2.92 ± 0.26	1.11 ± 0.17	0.92 ± 0.09
>40 yr	15	55.5 ± 11.7	12.4 ± 14.5	2.90 ± 0.48	0.97 ± 0.14	0.76 ± 0.17
Significance			ns	ns	$p < 0.05$	$p < 0.05$
Gender						
Male	18	45.1 ± 17.4	7.8 ± 19.6	2.89 ± 0.36	1.17 ± 0.18	0.96 ± 0.10
Female	11	36.5 ± 15.1	10.1 ± 11.8	2.95 ± 0.44	0.96 ± 0.10	0.77 ± 0.14
Significance		ns	ns	ns	$p < 0.005$	$p < 0.005$

WR = washout rate; H/M = heart-to-mediastinum count ratio; I/A = inferior-to-anterior wall count ratio.

washout rate or the heart-to-mediastinum count ratio, the inferior-to-anterior wall count ratio was lower for men than women on both planar images (0.96 ± 0.10 versus 1.17 ± 0.18; $p < 0.005$) and SPECT images (0.77 ± 0.14 versus 0.96 ± 0.10; $p < 0.005$) (Table 3).

Figure 4 shows the correlation of the MIBG parameters with age in men and women. No significant correlations were observed between the heart-to-mediastinum count ratio and age ($r = 0.06$; p = ns) or between the washout rate and age ($r = 0.26$; p = ns). On the other hand, the inferior-to-anterior wall count ratio showed an inverse correlation with age in both the planar images ($r = -0.51$; $p < 0.01$) and the SPECT study ($r = -0.69$; $p < 0.001$). These correlations were more striking in the men ($r = -0.74$ and $r = -0.83$ respectively; both $p < 0.001$) than in the women ($r = -0.25$ and -0.34 respectively; both p = ns).

DISCUSSION

This study demonstrates reduced [^{123}I]MIBG uptake in older individuals, particularly in men, indicating an age- and gender-related reduction of adrenergic neuronal function in the inferior myocardium of normal individuals. Since [^{123}I]MIBG uptake in the whole myocardium and tracer washout did not change with age or gender, regional heterogeneity may be striking in both older subjects and male subjects rather than a change of total myocardial neuronal function.

Noninvasive imaging with radioiodinated MIBG can assess efferent adrenergic neuronal function in the heart (*1–5*). MIBG competes with norepinephrine for neuronal uptake (uptake-1) (*23,24*) and is also taken up by a low-affinity non-neuronal mechanism (uptake-2) (*25–27*). Denervated myocardium with epicardial phenol application (*28*) and stellate ganglionectomy (*27*) showed a decrease in tissue norepinephrine and MIBG in the myocardium as well. These experimental data indicate that MIBG uptake may reflect adrenergic neuronal function accurately in the myocardium in vivo. Furthermore, radiolabeling with ^{123}I facilitates the use in clinical settings with a standard gamma camera, as documented in a variety of patient studies (*6–18*).

Although this study included both normal subjects and patients with malignant diseases, none of them had cardiac, pulmonary or mediastinal involvements. Furthermore, this study demonstrated a significant relationship between heterogenous MIBG uptake and subject age. Heterogeneity of MIBG distribution was frequently observed in our routine studies and thus caused difficulties in image interpretation. Data reported by Sisson et al. (*6*) suggest that there is reduced MIBG uptake at the cardiac apex, whereas Kline et al. (*1*) found reduced uptake at the septum. Gill et al. (*15*) studied normal subjects and found that the MIBG map of sympathetic catecholaminergic nerve terminals in the myocardium is normally inhomogeneous with a relative decrease in the inferior and septal regions. Our data correlate with Gill et al.'s for older subjects, but our results from the younger normal subjects showed more homogeneous MIBG distribution. Schwaiger et al. (*9*) reported similar homogeneous distribution in a PET study using ^{11}C-hydroxyephedrine performed on subjects with a mean age of 23 yr. These data indicate that the sympathetic neuronal function of the inferior wall may be decreased in older men, leading to heterogeneity of MIBG distribution in the myocardium.

Several possible explanations for this finding can be considered. Previous animal studies have demonstrated that the anterior wall of the left ventricle has a predominantly sympathetic afferent innervation, that the inferior wall has a predominantly parasympathetic innervation (*30–32*) and that such differences may cause a reduction of sympathetic neuronal function in the inferior region; however, the heterogeneity of sympathetic innervation or catecholamine levels in the human myocardium has not yet been determined. Another possibility is that the increase of plasma catecholamine levels with aging (*30,33,34*) may disturb myocardial sympathetic neuronal function, particularly in the inferior region, which might be more sensitive than other regions.

On the other hand, our results did not show a significant decrease in MIBG uptake in the whole myocardium or washout from the myocardium. Sympathetic neuronal

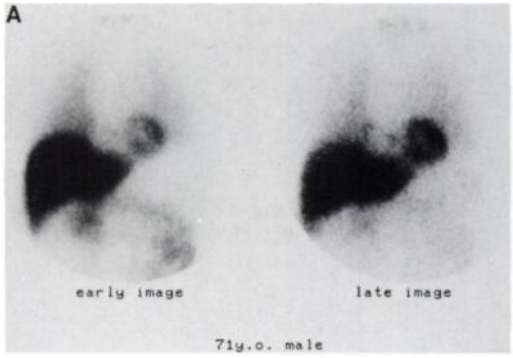

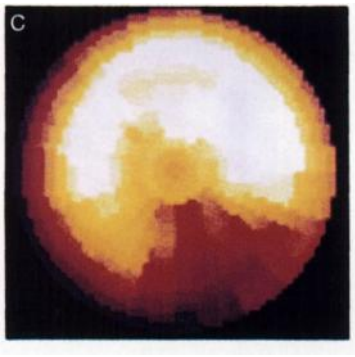

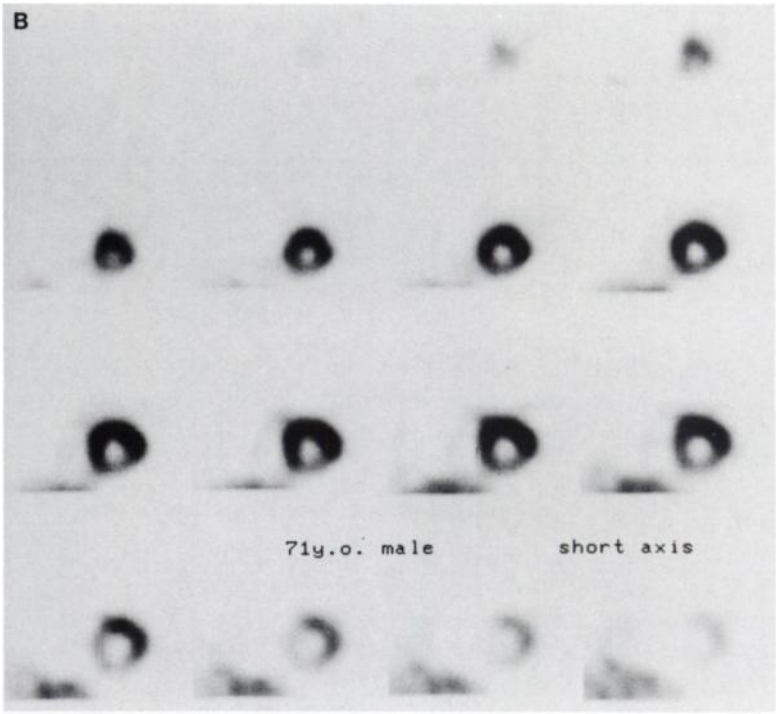

FIGURE 2. A 71-yr-old man with malignant lymphoma before adriamycin administration. High accumulation of tracer in the myocardium is shown on the early and the late planar images (A). On the short-axis images (B) and bull's-eye polar map (C), however, decreased MIBG uptake in the inferior region is noted.

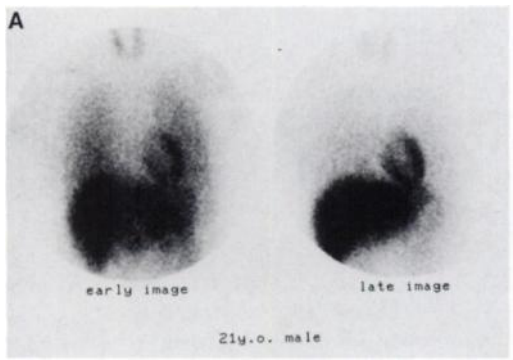

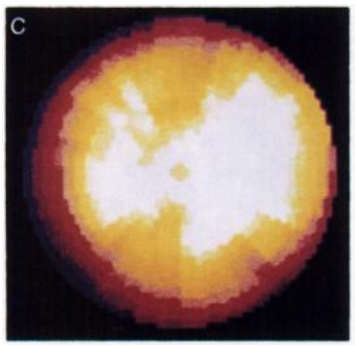

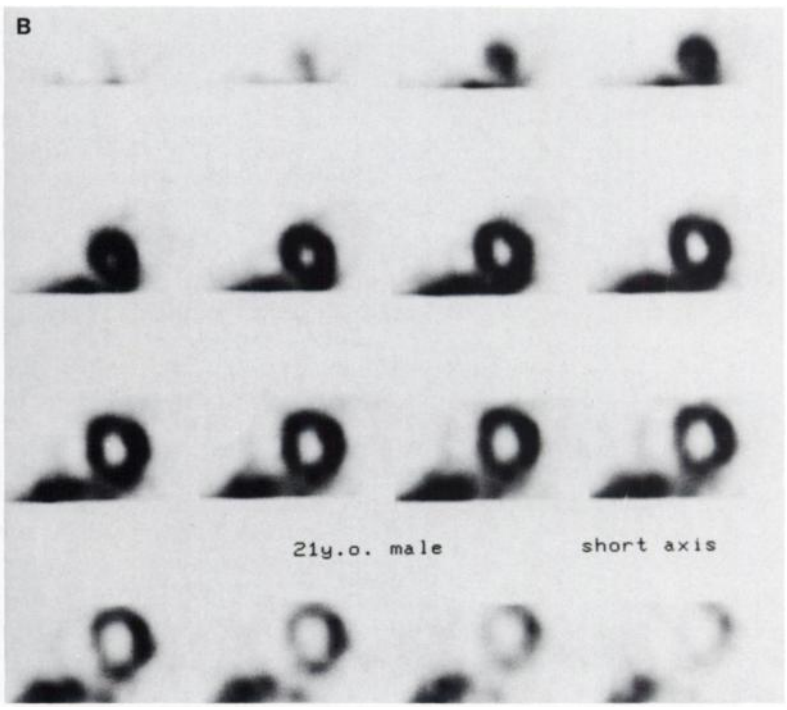

FIGURE 3. A 21-yr-old normal male volunteer. A high accumulation of the tracer in the myocardium is shown on the early and the late planar images (A). On short-axial images (B) and the bull's-eye polar map (C), there is almost homogenous distribution in the myocardium.

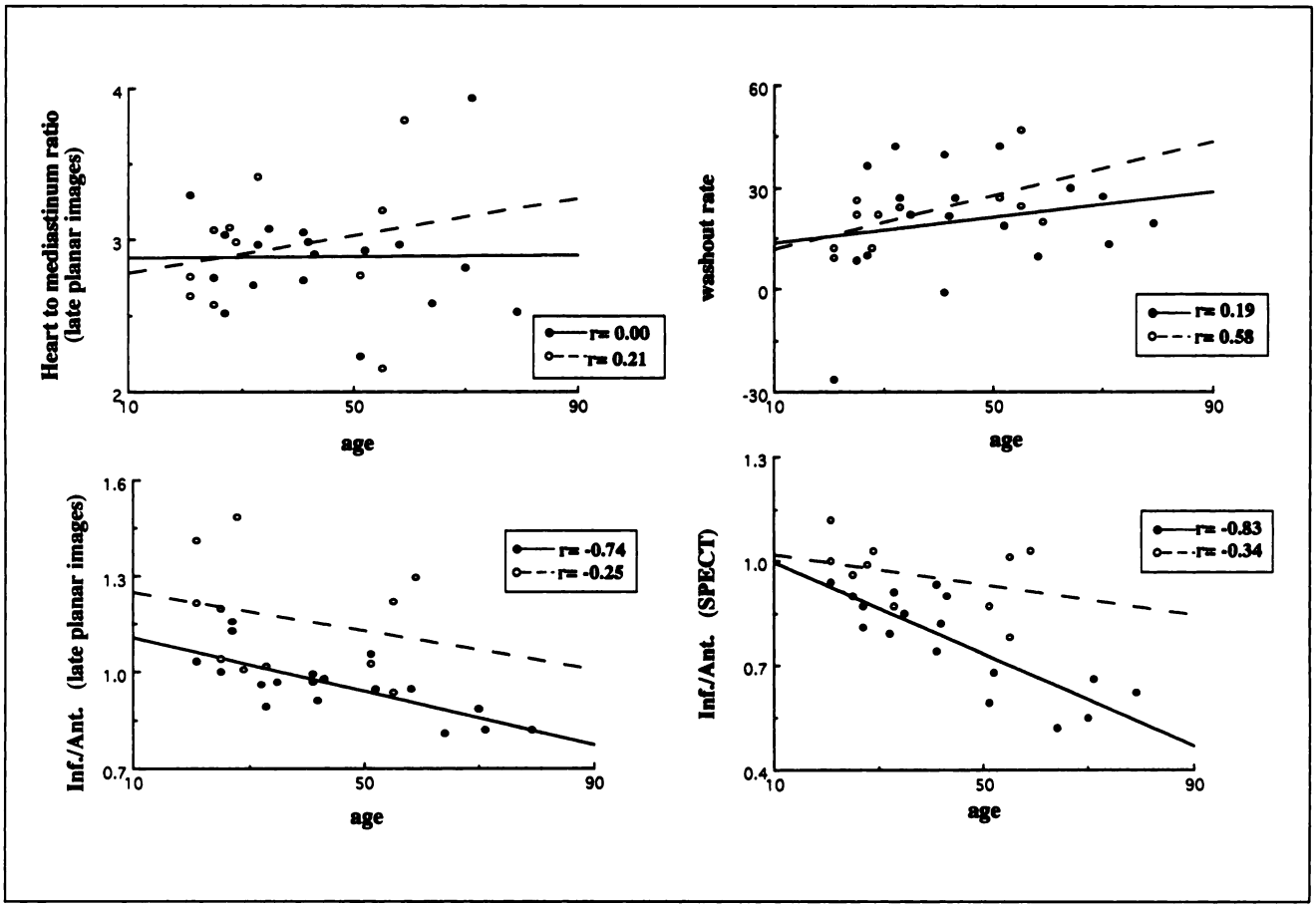

FIGURE 4. Correlation of various MIBG parameters according to age (closed circle = men; open circle = women).

function in the inferior region may be selectively disturbed with an increase in plasma catecholamine levels; however, we did not measure plasma catecholamine levels in each subject. Another study is warranted to compare plasma catecholamine levels with age or inferior-to-anterior wall count ratio in the normal subjects.

It is also important for potential artifacts to be considered. Diaphragmatic attenuation may cause a regional decrease of activity in the inferior wall on thallium and MIBG images, and this may contribute to gender differences in tracer distribution in the anterior and inferior regions; however, ^{123}I photons have a higher energy than thallium photons, so there should be less attenuation. In addition, there have been no reports indicating an age-related difference in diaphragmatic attenuation. Differences in the degree of rotation may also cause a differential sensitivity in the detection of inferior and lateral abnormalities (*35*), but all the subjects were scanned using the same 180° rotation protocol in our study. A recent report suggested that a high uptake in the liver may cause an artificial decrease in the inferior myocardial counts (*36*), but the activity in the liver did not change with age or gender in our study. Such a potential artifact did not explain our age- and gender-related differences in MIBG heterogeneity in the myocardium.

CONCLUSION

In subjects without cardiac disorders, MIBG uptake in the inferior region gradually reduced with age, particularly in the male subjects. Such heterogeneity of myocardial sympathetic innervation in normal subjects may cause difficulties when interpreting MIBG images. For better interpretation of MIBG images, careful consideration of physiologic change in sympathetic neuronal function with age and gender is important.

ACKNOWLEDGMENTS

The authors thank Emiko Komori, RT, and Seiji Shirakawa, RT, for technical assistance and Daiichi Radioisotope Laboratories Ltd. for supplying [^{123}I]MIBG.

REFERENCES

1. Kline RC, Swanson DP, Wieland DM, et al. Myocardial imaging in man with I-123 meta-iodobenzylguanidine. *J Nucl Med* 1981;22:129–132.
2. Sisson JC, Frager MS, Valk TW, et al. Scintigraphic localization of pheochromocytoma. *N Eng J Med* 1981;305:12–17.
3. Shapiro B, Sisson JC, Lloyd R, Nakajo M, Satterlee W, Beierwalts WH. Malignant pheochromocytoma: clinical, biochemical and scintigraphic characteristics. *Clin Endocrinol* 1984;20:189–203.
4. Lynn MD, Shapiro B, Sisson JC, et al. Portrayal of pheochromocytoma and normal human medulla by m-(^{123}I)iodobenzylguanidine: concise communication. *J Nucl Med* 1984;25:436–440.
5. Kimmig B, Brandeis WE, Eisenhut M, Bubeck B, Hermann HJ, zum-

Winkel K. Scintigraphy of a neuroblastoma with I-131 meta-iodobenzylguanidine (I-131-MIBG). *J Nucl Med* 1984;25:773–775.
6. Sisson JC, Shapiro B, Meyers LJ, et al. Meta-iodobenzylguanidine to map scintigraphically the adrenergic nervous system in man. *J Nucl Med* 1987; 28:1625–1636.
7. Stanton M, Tuli M, Radtke N, et al. Regional sympathetic denervation after myocardial infarction in humans detected non-invasively using I-123 meta-iodobenzylguanidine. *J Am Coll Cardiol* 1989;14:1519–1526.
8. McGhie AI, Corbett JR, Akers MS, et al. Regional cardiac adrenergic function using I-123 meta-iodobenzylguanidine tomographic imaging after acute myocardial infarction. *Am J Coll Cardiol* 1991;67:236–242.
9. Dae MW, Herre JM, O'Connell W, Botvinick EH, Newman D, Munoz L. Scintigraphic assessment of sympathetic innervation after transmural versus non-transmural myocardial infarction. *J Am Coll Cardiol* 1991;17:1416–1423.
10. Henderson EB, Kahn JK, Corbett JR, et al. Abnormal I-123 metaiodobenzylguanidine myocardial washout and distribution may reflect myocardial adrenergic derangement in patients with congestive cardiomyopathy. *Circulation* 1988;78:1192–1199.
11. Nakajima K, Bunko H, Taki J, Shimizu M, Muramori A, Hisada K. Quantitative analysis of ^{123}I-meta-iodobenzylguanidine (MIBG) uptake in hypertrophic cardiomyopathy. *Am Heart J* 1990;119:1329–1337.
12. Wieland DM, Wu j, Brown LE, Mangner TJ, Swasson DP, Beierwaltes WH. Radiolabeled adrenergic neuron-blocking agent: adrenomedullary imaging with [^{131}I] iodobenzylguanidine. *J Nucl Med* 1980;21:349–353.
13. Glowniak JV, Turner FE, Gray LL, et al. Iodine-123 meta-iodobenzylguanidine imaging of the heart in idiopathic congestive cardiomyopathy and cardiac transplants. *J Nucl Med* 1989;30:1182–1191.
14. Dae MW, Marco TD, Botvinick EH, et al. Scintigraphic assessment of MIBG uptake in globally denervated human and canine hearts—implications for clinical studies. *J Nucl Med* 1992;33:1444–1450.
15. Gill JS, Hunter JG, Gane J, Ward DE, Camm AJ. Asymmetry of cardiac (^{123}I) meta-iodobenzylguanidine scans in patients with ventricular tachycardia and a "clinically normal" heart. *Br Heart J* 1993;69:6–13.
16. Rabinovitch MA, Rose CP, Schwab AJ, et al. A method of dynamic analysis of iodine-123-meta-iodobenzylguanidine scintigrams in cardiac mechanical overload hypertrophy and failure. *J Nucl Med* 1993;34:589–600.
17. Shakeapeare CF, Page CJ, O'Doherty MJ, et al. Regional sympathetic innervation of the heart by means of meta-iodobenzylguanidine imaging in silent ischemia. *Am Heart J* 1993;125:1614–1622.
18. Fagret D, Wolf JE, Vanzetto G, Borrel E. Myocardial uptake of meta-iodobenzylguanidine in patients with left ventricular hypertrophy secondary to valvular aortic stenosis. *J Nucl Med* 1993;34:57–60.
19. Gill JS, Hunter GJ, Gane G, Camm AJ. Heterogeneity of the human myocardial sympathetic innervation: in vivo demonstration by iodine-123-labeled meta-iodobenzylguanidine scintigraphy. *Am Heart J* 1993;126:390–398.
20. Tamaki N, Yonekura Y, Mukai T, et al. Stress thallium-201 transaxial emission computed tomography; quantitative versus qualitative analysis for evaluation of coronary artery disease. *J Am Coll Cardiol* 1984;4:1213–1221.
21. Garcia EV, Van Train K, Maddahi J, et al. Quantification of rotational thallium-201 myocardial tomography. *J Nucl Med* 1985;26:17–26.
22. Merlet P, Valette H, Dubois-Rande JL, et al. Prognostic value of cardiac meta-iodobenzylguanidine imaging in patients with heart failure. *J Nucl Med* 1992;33:471–477.
23. Slosman DO, Davidson D, Brill AB, Alderson PO. Iodine-131-meta-iodobenzylguanidine uptake in the isolated rat lung: a potential marker of endothelial cell function. *Eur J Nucl Med* 1988;13:543–547.
24. Nakajo M, Shapiro B, Glowniak J, Sisson JC, Beiermaltes WH. Inverse relationship between cardiac accumulation of meta-[^{131}I]iodobenzylguanidine (I-131 MIBG) and circulating catecholamines in suspected pheochromocytoma. *J Nucl Med* 1983;24:1127–1134.
25. Nakajo M, Shimabukuro K, Yoshimura H, et al. Iodine-131 meta-iodobenzylguanidine intra- and extravesicular accumulation in the rat heart. *J Nucl Med* 1986;27:84–89.
26. Sisson JC, Wieland DM, Sherman P, Mangner TJ, Tobes MC, Jacques S Jr. Meta-iodobenzylguanidine as an index of the adrenergic nervous system integrity and function. *J Nucl Med* 1987;28:1620–1624.
27. Dae MW, O'Connell W, Botvinick E, et al. Scintigraphic assessment of regional cardiac adrenergic innervation. *Circulation* 1989;79:634–644.
28. Sisson JC, Lynch JJ, Johnson J, et al. Scintigraphic detection of regional disruption of adrenergic neurons in the heart. *Am Heart J* 1988;116:67–76.
29. Schwaiger M, Kalff V, Rosenspire K, et al. Noninvasive evaluation of sympathetic nervous system in human heart by positron emission tomography. *Circulation* 1990;82:457–464.
30. Weaver LC, Danos LM, Oehl RS, Meckler RL. Contrasting reflex influences of cardiac afferent nerves during coronary occlusion. *Am J Physiol* 1981;240:620–629.
31. Thames MD, Klopfenstein HS, Abbound FM, Mark AL, Walker JL. Preferential distribution of inhibitory cardiac receptors with vagal afferents to the inferoposterior wall of the left ventricle activated during coronary occlusion in the dog. *Circ Res* 1978;43:512–519.
32. Pantridge JF. Autonomic disturbances at the onset of acute myocardial infarction. In: Schwartz P, Brown AM, Malliani A, Zanchetti A, eds. *Neuronal mechanisms in cardiac arrhythmias*. New York: Raven Press; 1978:7–17.
33. Randall W, Armour JA, Geis P, Lippencott D. Regional cardiac distribution of sympathetic nerves. *Fed Proc* 1972;31:199–208.
34. Dahlstrom A, Fuxe K, Mya-Tu M, Zetterstrom BEM. Observations on adrenergic innervation of dog heart. *Am J Physiol* 1965;209:689–692.
35. Maublant JC, Peycelon P, Kwiatkowski F, Lusson JR, Standkuia R, Veyre A. Comparison between 180 degree and 360 degree data collection in technetium-99m MIBI SPECT of the myocardium. *J Nucl Med* 1989;30:295–300.
36. Germano G, Chua T, Kiat H, Areeda JS, Berman DS. A quantitative phantom analysis of artifacts due to hepatic activity in technetium-99m myocardial perfusion SPECT studies. *J Nucl Med* 1994;35:356–359.